A comparison of high-order time integrators for highly supercritical thermal convection in rotating spherical shells

F. Garcia, M. Net and J. Sánchez

Abstract The efficiency of implicit and semi-implicit time integration codes based on backward differentiation and extrapolation formulas for the solution of the three-dimensional Boussinesq thermal convection equations in rotating spherical shells was studied in [6] at weakly supercritical Rayleigh numbers R, moderate (10^{-3}) and low (10^{-4}) Ekman numbers, E, and Prandtl number $\sigma = 1$. The results presented here extend the previous study and focus on the effect of σ and R by analyzing the efficiency of the methods for obtaining solutions at $E = 10^{-4}$, $\sigma = 0.1$ and low and high supercritical R. In the first case (quasiperiodic solutions) the decrease of one order of magnitude does not change the results significantly. In the second case (spatio-temporal chaotic solutions) the differences in the behavior of the semi-implicit codes due to the different treatment of the Coriolis term disappear because the integration is dominated by the nonlinear terms. As in [6], high order methods, either with or without time step and order control, increase the efficiency of the time integrators and allow to obtain more accurate solutions.

1 Introduction

Thermal convection in rotating spherical geometries dominates the dynamics of several astrophysical and geophysical phenomena such as the generation of the magnetic field exhibited by celestial bodies or the cloud patterns and the differential rotation seen at the surface of the major planets.

There are several experimental and numerical difficulties in the study of thermal convection in spherical geometry. In the first case, the radial gravity can be reproduced by means of either an electrostatic radial field or by the centrifugal force. In

F. Garcia · M. Net · J. Sánchez
Departament de Física Aplicada, Universitat Politènica de Catalunya, Jordi Girona Salgado s/n, Campus Nord. Mòdul B4, 08034 Barcelona, Spain, e-mail: ferran@fa.upc.edu, marta@fa.upc.edu, sanchez@fa.upc.edu

the second case non-stationary tridimensional waves arise at the onset of convection due to the boundary curvature, and thus finding a solution requires very high resolutions. Frequently, as in [12], and [13], a two-dimensional annular geometry is used to approximate the real problem.

Due to the increase of the computing power, many numerical papers, [8, 18, 4, 17] among others, most of them based on pseudo-spectral methods and second order time integration, have been published. The most exhaustive tridimensional studies consist of numerical evolutions of periodic, quasi-periodic, and even turbulent flows, mainly with stress-free boundary conditions to avoid the formation of Ekman layers. These boundary conditions are inappropriate for comparison with laboratory studies and to model systems like the Earth's outer core, where thin Ekman boundary-layers exist near the rigid boundaries.

For a deeper understanding of the origin of the laminar flows and their dependence on parameters, pseudoarclength continuation methods [15, 16], and the linear stability analysis of the time dependent solutions [11, 7] have been successfully applied thanks to the use of high-order time integration methods which provide accurate enough solutions. On the other hand, high-order time integration can be also useful for evolving turbulent flows efficiently.

The performance of several high order implicit-explicit (IMEX) schemes, including those based on backward differentiation formulae (BDF), were exhaustively studied in [2] for the linear advection-diffusion one-dimensional problem. A stability analysis of the multistep methods up to fourth order were also performed. In that study the diffusive term is taken implicitly and the advection term explicitly. For the IMEX-BDF schemes, they showed that larger time-steps are allowed for the second order scheme when diffusion dominates the dynamics. In contrast, the third and fourth-order schemes can take larger time-steps when the explicit advection term becomes relevant. In addition, and in contrast to the widely used second order Crank-Nicolson and Adams-Bashforth scheme (CNAB2), the authors of [2] argued that IMEX-BDF methods are useful for reducing the aliasing effects when using pseudo-spectral methods [3], due to the strong damping of the high frequency modes, which appear when computing the nonlinear terms. Other similar class of IMEX methods with better stability regions are those based on Runge-Kutta (RK) schemes [1]. However, when compared with the multistep BDF, RK-based methods would require one additional nonlinear evaluation for each stage. This is not affordable in problems for which the evaluation of the nonlinear part is the most demanding task.

The efficiency of different time integration methods to solve the thermal convection equations in rotating spherical shells was studied in [6]. The same IMEX-BDF time integration pseudo-spectral codes, with the nonlinear terms of the equations taken explicitly in order to avoid solving nonlinear equations at each time step, are used in this study. The Coriolis term is treated either semi-implicitly or fully implicitly, giving rise to the different algorithms analyzed. The use of iterative methods facilitates the implementation of a suitable order and time stepsize control.

Two periodic solutions, of different E (the rest of parameters are the same) were integrated in [6] to highlight the influence of the Ekman number. Extending the

previous study, a periodic and a quasiperiodic solution, computed with different σ are integrated to address the Prandtl number influence. In addition, by only varying the Rayleigh number, the efficiency of the time integration methods is studied when considering a spatio-temporal chaotic solution.

The rest of the article is organized as follows. In Section 2, the formulation of the problem and the spatial discretization of the equations are introduced. In Section 3, the time discretization schemes are described briefly. In Section 4 the differences between the constant stepsize methods are shown, and the study of the implicit and semi-implicit variable stepsize and variable order methods is reported. Finally, the paper closes in Section 5 with a brief summary of the main conclusions.

2 Mathematical model and spatial discretization

The thermal convection of a spherical fluid shell differentially heated, rotating about an axis of symmetry with constant angular velocity $\Omega = \Omega\mathbf{k}$, and subject to radial gravity $\mathbf{g} = -\gamma\mathbf{r}$, where γ is a constant, and $\mathbf{r}$ the position vector, is considered. The mass, momentum and energy equations are written by using the same formulation and non-dimensional units as in [11]. The units are the gap width, $d = r_o - r_i$, for the distance, $\nu^2/\gamma\alpha d^4$ for the temperature, and d^2/ν for the time, ν being the kinematic viscosity, α the thermal expansion coefficient, and r_i and r_o the inner and outer radii, respectively. The velocity field $\mathbf{v}$ is expressed in terms of toroidal, Ψ, and poloidal, Φ, scalar potentials $\mathbf{v} = \nabla\times(\Psi\mathbf{r}) + \nabla\times\nabla\times(\Phi\mathbf{r})$, and $\Theta = T - T_c$ is the temperature perturbation from the conduction state $\mathbf{v} = \mathbf{0}$, $\quad T_c(r) = T_0 + R\eta/\sigma(1-\eta)^2 r$, with $r = ||\mathbf{r}||_2$.

With the functions $X = (\Psi, \Phi, \Theta)$ expanded in spherical harmonic series up to degree L, the equations written for their complex coefficients are

$$\partial_t \Psi_l^m = \mathscr{D}_l \Psi_l^m + \tfrac{1}{l(l+1)}\left[2E^{-1}\left(im\Psi_l^m - [Q\Phi]_l^m\right) - [\mathbf{r}\cdot\nabla\times(\mathbf{w}\times\mathbf{v})]_l^m\right], \quad (1)$$

$$\partial_t \mathscr{D}_l \Phi_l^m = \mathscr{D}_l^2 \Phi_l^m - \Theta_l^m + \tfrac{1}{l(l+1)}\left[2E^{-1}\left(im\mathscr{D}_l\Phi_l^m + [Q\Psi]_l^m\right) + [\mathbf{r}\cdot\nabla\times\nabla\times(\mathbf{w}\times\mathbf{v})]_l^m\right], \quad (2)$$

$$\partial_t \Theta_l^m = \sigma^{-1}\mathscr{D}_l\Theta_l^m + \sigma^{-1}l(l+1)R\eta(1-\eta)^{-2}r^{-3}\Phi_l^m - [(\mathbf{v}\cdot\nabla)\Theta]_l^m, \quad (3)$$

with boundary conditions

$$\Psi_l^m = \Phi_l^m = \partial_r\Phi_l^m = \Theta_l^m = 0, \quad (4)$$

corresponding to non-slip perfect thermally conducting boundaries, and where $\mathbf{w} = \nabla\times\mathbf{v}$ is the vorticity field.

The spherical harmonic coefficients of the operator $Q = Q^u + Q^l$ are

$$[Q^u f]_l^m = -l(l+2)c_{l+1}^m D_{l+2}^+ f_{l+1}^m, \quad [Q^l f]_l^m = -(l-1)(l+1)c_l^m D_{1-l}^+ f_{l-1}^m, \quad (5)$$

with $D_l^+ = \partial_r + \frac{l}{r}$, $c_l^m = \left(\frac{l^2-m^2}{4l^2-1}\right)^{1/2}$, and $\mathscr{D}_l = \partial_{rr}^2 + \frac{2}{r}\partial_r - \frac{l(l+1)}{r^2}$.

The governing parameters are the Rayleigh number R, the Prandtl number σ, the Ekman number E, and the radius ratio η. They are defined by

$$R = \frac{\gamma\alpha\Delta T d^4}{\kappa\nu}, \quad E = \frac{\nu}{\Omega d^2}, \quad \sigma = \frac{\nu}{\kappa}, \quad \eta = \frac{r_i}{r_o},$$

where κ is the thermal diffusivity, and ΔT the difference of temperature between the inner and outer boundaries.

The coefficients of the nonlinear terms of equations (1-3) are obtained following [8]. In the radial direction, a collocation method on a Gauss-Lobatto mesh of N_r+1 points is employed (N_r-1 being the number of inner points). A large system of $N = (3L^2+6L+1)(N_r-1)$ ordinary differential equations must be advanced in time.

3 Time integration methods

The time integration methods used in this paper were described in detail in [6] so only the main ideas are exposed in the following. In order to simplify the notation, equations (1-3) are written in the form

$$\mathscr{L}_0\dot{u} = \mathscr{L}u + \mathscr{N}(u),$$

where $u = (\Psi_l^m(r_i), \Phi_l^m(r_i), \Theta_l^m(r_i))$, and $\mathscr{L}_0$ and $\mathscr{L}$ are linear operators including the boundary conditions. The former is invertible, and the latter, for any of the schemes used, includes the diffusive, the buoyancy, and part of the Coriolis terms to be specified below. The operator $\mathscr{N}$, which will be treated explicitly in the IMEX-BDF formulae, will always contain the nonlinear terms, and the rest of the Coriolis terms.

The IMEX-BDF formulae mentioned before are related to the BDF [5]. They obtain $u^{n+1} \approx u(t_{n+1})$ on a given time level t_{n+1}, $n = 0,1,2,\ldots,$ from the previous approximations u^{n-j}, $j = 0,1,\ldots,k-1$, using the following k-steps formula

$$\left(\mathscr{I} - \frac{\Delta t_n}{\gamma_0(n)}\mathscr{L}_0^{-1}\mathscr{L}\right)u^{n+1} = \frac{\Delta t_n}{\gamma_0(n)}\mathscr{L}_0^{-1}p_{n,k-1}(t_{n+1}) - \frac{\dot{q}_{n,k}^0(t_{n+1})}{\dot{l}_{n,k}(t_{n+1})}, \qquad (6)$$

where $q_{n,k}^0(t) = q_{n,k}(t) - u^{n+1}l_{n,k}(t)$, being $q_{n,k}$ the interpolating polynomial of degree at most k, such that $q_{n,k}(t_{n-j}) = u^{n-j}$, for $j = -1,0,\ldots,k-1$, and $l_{n,k}$ the polynomial of degree at most k taking the value 1 at t_{n+1}, and 0 at t_{n-j}, for $j = 0,1,\ldots,k-1$. Moreover $p_{n,k-1}$ is the interpolating polynomial of degree at most $k-1$, such that $p_{n,k-1}(t_{n-j}) = \mathscr{N}(u^{n-j})$, for $j = 0,1,\ldots,k-1$, $\mathscr{I}$ is the identity

operator, and $\gamma_0(n) = \dot{l}_{n,k}(t_{n+1})\Delta t_n$, being $\Delta t_n = t_{n+1} - t_n$, $n = 0, 1, 2, \ldots,$ the time step.

If the time step is constant, the IMEX-BDF formulae (6) reduces to

$$\left(\mathscr{I} - \frac{\Delta t}{\gamma_0}\mathscr{L}_0^{-1}\mathscr{L}\right) u^{n+1} = \sum_{i=0}^{k-1} \frac{\alpha_i}{\gamma_0} u^{n-i} + \sum_{i=0}^{k-1} \frac{\beta_i \Delta t}{\gamma_0} \mathscr{L}_0^{-1}\mathscr{N}(u^{n-i}), \qquad (7)$$

where the coefficients α_i, β_j and γ_0 do not depend on n, and are listed, for instance, in [15]. In this case the matrix of the system to be solved does not change with n. On the other hand, changing the stepsize allows the use of formulas of different orders (step numbers) k, while maintaining accuracy. Then the integration can be started with $k = 1$ (and small Δt_0), when the lack of previously computed values precludes the use of higher order formulas, and then increase the order (and the step length) as the integration advances and previous approximations u^{n-j} are available. For the fixed-step-size codes, the starting values u^j, $j = 1, \ldots, k-1$ are obtained by time integration from t_{j-1} to t_j with a VSVO (variable step-size variable order) code with sufficiently small tolerances ε^a and ε^r, which are, respectively, the tolerances below which the absolute and relative values of the local (time discretization) errors are required. The local error control of the IMEX VSVO methods is performed as usual, i.e. following [9]. If a time step is selected giving a point outside the stability region, the accumulation of local errors will enforce the method to select smaller time steps to ensure the stability. Details on the strategy carried out to control the stepsize and the order of the VSVO codes, such as the estimations of the local error of the k-order formula, are outlined in [6].

Once the nonlinear terms are evaluated, equations (1-3) decouple for each azimuthal wave number m, thus, at every time step, $L+1$ linear systems of the form $H^m U^m = V^m, \quad m = 0, ..., L,$ have to be solved. The vectors U^m and V^m contain, respectively, the unknowns and the right hand side of the linear system derived from the IMEX-BDF formulae (6) or (7), with azimuthal wave number m. The dimension of the matrices H^m is $6(L-m+1)(N_r-1)$ and its structure depends on which terms of equations (1-3) are treated implicitly (see the Appendix A of [6] for further details).

The inclusion of the diagonal parts of the Coriolis term containing $im\Psi_l^m$ and $im\Phi_l^m$ in $\mathscr{L}$, and of Q in $\mathscr{N}$, gives block-diagonal matrices H^m, with blocks of dimension $6(N_r-1)$. The solution of these linear systems is performed by a direct LU method. From now on, the time discretization with this treatment of the operators will be called the Q-explicit method.

By adding Q^u or Q^d (see Eq. 5) to $\mathscr{L}$, the matrices H^m become upper or lower block-triangular matrices, respectively. They can be solved, with the same memory requirements and number of operations than the Q-explicit method, by using backward or forward block substitution. In order to implement this possibility in a symmetric way, the two options are used alternately, that is, one step is performed with Q^u implicit and Q^d explicit, and vice-versa in the following step. From now on, this time discretization will be called the Q-splitting method.

By setting Q totally implicit the operator $\mathscr{N}$ only includes the nonlinear terms, and then the matrices H^m become block-tridiagonal. From now on this method will be called the Q-implicit method. A direct block method for solving these linear systems involves about three times the memory storage required for solving the block-diagonal systems, and at least three times the computational cost of performing the LU decomposition. As the solution of the linear systems is not the most demanding task to advance one time step, we decided to solve it iteratively without storing the matrices to cope with higher resolutions, and to implement a variable size and order version, which requires updating the LU factorizations. Iterative methods based on Krylov techniques, can be used efficiently, if they are preconditioned with the block diagonal matrix. We have chosen the GMRES method because it is suitable for non-symmetric linear systems and it has good convergence properties [14]. The initial approximation for solving the linear system is obtained by extrapolation from the previous steps. The increase in the cost of solving the linear systems may be offset by the increase of the time stepsize.

The integration with a constant time step can be unnecessarily expensive because the step must be short enough to cope with possible fast transients. To avoid this situation, a refined procedure is to use a VSVO method [9]. In the derivation of the VSVO IMEX-BDF formula, the matrices of the linear systems depend on the current time step. They can be solved efficiently, if a Krylov method with a preconditioning matrix depending on a fixed time step Δt^* is used. When the convergence of the iterative linear solver degrades doing more than 10 iterations, the preconditioning matrix can be updated with the current time step instead of restarting. In the case of the VSVO methods the tolerance for the GMRES residual is asked to be two orders of magnitude lower than that required for the time integration. The rate of convergence depends on the order k and the time step. For example, when integrating with low order $k = 2$ it converges in about 6-10 iterations, while with $k = 5$ only 2 iterations are required. All the semi-implicit methods described before have been implemented with constant time-step size, and with variable time-step size and order using our own codes (except the Q-splitting VSVO method). From now on, the VSVO implementations of the Q-explicit and Q-implicit methods will be called Q-explicit VSVO and Q-implicit VSVO, respectively.

The last option considered is a fully implicit treatment of the nonlinear terms with a VSVO formulation of the BDF. This leads to the solution of a nonlinear system of equations at each step. This solution is obtained by means of a Newton-Krylov method using GMRES to solve the Newton correction equations with zero initial seed, see [10] for further details. From now on this method will be called fully implicit method. We will use the DLSODPK code of the ODEPACK package [10]. The linear systems to be solved in this case depend not only on the current time step, but also on the current solution. As before, they can be preconditioned by the block-diagonal matrices computed with a fixed time step Δt^*. If during the integration the current time step is different from Δt^* by one order of magnitude the preconditioner is recomputed with the current time step. As in the semi-implicit VSVO methods, the tolerance imposed on the residuals depends on the tolerance imposed on the

time integration. The cost of the nonlinear evaluations performed to approximate the Jacobian matrix products degrade the performance of the fully implicit methods.

4 Results

To study the effect of the Prandtl number σ and the Rayleigh number R on the efficiency of the time integration schemes presented in the previous section, we integrate three different cases with $\eta = 0.35$ and $E = 10^{-4}$. The first one (case S_1) was studied in [6] (there called C_2) and corresponds to a periodic traveling wave of wave number $m = 7$, computed at $\sigma = 1$ and $R = 800000$. In the second case (S_2) we integrate a quasiperiodic three frequency wave with $m = 6$ computed at smaller Prandtl number $\sigma = 0.1$ and $R = 264000$. On both cases R is slightly supercritical and the solutions are quasi-geostrophic and symmetric with respect to the equator. Finally, a highly supercritical spatio-temporal chaotic solution, computed with $\sigma = 0.1$ and $R = 2000000$, is considered for the third case (S_3). The numerical resolutions employed for the S_1, S_2 and S_3 cases are, $N_r = 48$ and $L = 63$ ($N = 577442$ equations), $N_r = 32$ and $L = 54$ ($N = 281263$ equations), and $N_r = 50$ and $L = 84$ ($N = 1083650$ equations), respectively.

To make our comparisons the initial transient has been discarded, and all the test runs are started with the same initial condition obtained after the solution has smoothed. To obtain it, the Q-implicit VSVO method with very low tolerances was used. Then the system (1-4) is evolved from the new initial condition to a final time t_f. In the S_1 and S_2 cases $t_f = 0.1$, while in the S_3 case $t_f = 0.01$.

To check the efficiency of the different schemes the relation between the relative error, and the run time is studied. The former is defined as

$$\varepsilon(u) = \frac{||u - u_r||_2}{||u_r||_2}, \tag{8}$$

where u is the solution we want to check, and u_r is an accurate reference solution obtained with the Q-implicit VSVO method. More precisely, u_r is obtained with tolerances $\varepsilon^a = \varepsilon^r$ equal to 10^{-13} in the S_1 and S_2 cases, and to 10^{-11} in the S_3 case. The decrease of the relative error (8) is achieved by decreasing the stepsize in the case of fixed stepsize methods, or by decreasing the tolerances for the local errors in the case of the VSVO methods.

For the constant time stepsize methods of orders 2 to 5 (except the Q-implicit method for the sake of simplicity) the relative error $\varepsilon(u)$ is plotted against the time step in Figs. 1(a,c,e). The efficiency curves are shown in Figs. 1(b,d,f). In the latter, $\varepsilon(u)$ is plotted against the run time in seconds for the results of the VSVO codes together with the constant stepsize Q-splitting method for comparison purposes. Plots (a) and (b), (c) and (d), and (e) and (f), are for the S_1, S_2, and S_3 cases, respectively.

As mentioned previously, the study of the S_1 case (Figs.1(a) and (b)) was performed in [6] so only a few words are commented here. For a given constant time

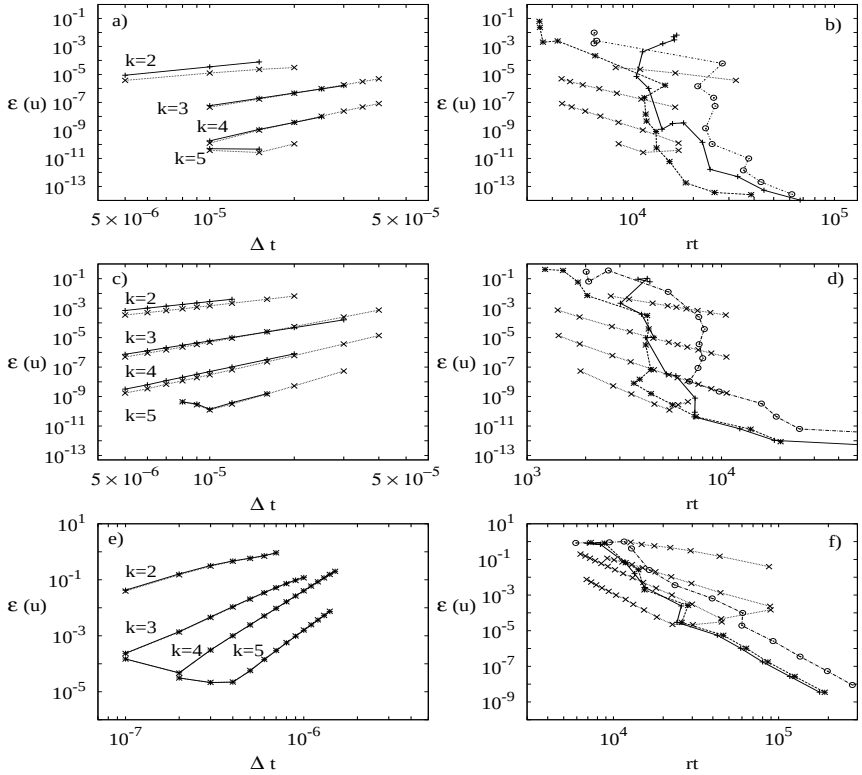

Fig. 1 (a) The relative error, $\varepsilon(u)$, plotted versus the time step Δt for constant time step integration, orders k from 2 to 5, and the S_1 case. (c), (e) Same as (a), for the S_2 and S_3 cases, respectively. (b) The relative error, $\varepsilon(u)$, plotted versus the run time for the Q-splitting and VSVO methods, and the S_1 case. (d), (f) Same as (c), for the S_2 and S_3 cases, respectively. The symbols mean: Q-explicit ($+$, solid line), Q-splitting ($\times$, dotted line), Q-explicit VSVO ($+$, solid line), Q-implicit VSVO ($*$, dashed line), and DLSODPK ($\circ$, dash-dotted line).

stepsize, the Q-explicit and the Q-splitting methods of all the orders have almost the same computational cost, and therefore the higher order methods should be preferred. In addition, the Q-splitting method has shown itself to be more stable, allowing for larger time steps (see Fig.1(a)), and hence, better efficiency. For the latter method, Fig. 1(b) shows that at approximately $\varepsilon(u) < 10^{-9}$, the order $k = 5$ is the most efficient but if $\varepsilon(u) > 10^{-9}$ the most efficient order is 4. The fully implicit method using DLSODPK is always more expensive than the Q-implicit VSVO methods because each iteration of the linear solver, and of the Newton's method requires an expensive evaluation of the non-linear terms. In all the results shown, it takes between 1 and 3 Newton iterations, and for each of them 1 or 2 GMRES iterations. The Q-explicit VSVO method is also less expensive than DLSODPK, except for the higher $\varepsilon(u)$, for which the cost of the former increases due to a decrease of the solver performance. The abrupt decrease of efficiency of the Q-implicit VSVO

method close to $\varepsilon(u) = 10^{-3}$ was related in [6] with the shape of the stability regions of the BDF for constant stepsizes. A similar result was found in [2] in the framework of the one dimensional linear advection-diffusion problem. When the implicit term dominates (as occurs with the *Q*-implicit method at weak supercritical conditions) second order IMEX-BDF schemes allow larger time-steps than those of third or fourth order. The decrease of efficiency prevents the *Q*-implicit VSVO method from being as efficient as the *Q*-splitting method in the region of intermediate errors. However, for the latter, some previous experiments have to be performed to determine the optimal time step.

The behavior of the methods for integrating the S_2 case (Figs.1(c) and (d)) is similar to that of the S_1 case, despite they are less accurate. Although their Prandtl numbers differ in one order of magnitude, the results seem reasonable because in both cases the solutions are smooth functions of time and, in all the methods, the terms of Eqs. (1-3) containing the Prandtl number are treated implicitly. However, for a given order, the error $\varepsilon(u)$ of the fixed step methods is almost two order of magnitude greater in the S_2 case. The same occurs for the VSVO methods. This differences could be due to S_2 being slightly more complicated, in the sense that it has two additional frequencies. Nevertheless, accurate solutions with $\varepsilon(u)$ down to 10^{-11} can be obtained in a reasonable time.

As expected, the accuracy for integrating the spatio-temporal chaotic solution of the S_3 case drastically decreases with respect to the other cases. This decrease is also due to the larger number of time steps needed by the methods to obtain the solution at the desired t_f. This is shown in Figs.1(e) and (f) where $\varepsilon(u)$ down to 10^{-5}, and 10^{-9}, can be obtained with the fixed step, or the VSVO methods, respectively. Apart from the accuracy, the behavior of the methods is clearly different to that exhibited in the previous cases, at weakly supercritical regimes, where the Ekman number controls the dynamics. At highly supercritical *R*, the Ekman number plays minor role and the way the Coriolis term is treated becomes less important. According to this, the results obtained with the fixed time step *Q*-explicit, and the *Q*-splitting methods are nearly the same (Fig.1(e)), and the same occurs for the results of the VSVO *Q*-explicit and *Q*-implicit methods. Since the solution is strongly nonlinear, the efficiency of the fully implicit VSVO method becomes comparable to the semi-implicit VSVO methods, and better than the low order fixed step methods (Fig.1(f)). As commented in [6] this is because the fully implicit method allows significantly larger time steps (nearly 3 times in this case), but which are computationally expensive. It is worth mentioning that in the S_3 case the VSVO methods obtain solutions up to four orders of magnitude more accurate than the fixed time methods, while in the previous cases with the VSVO methods the improvement is of two orders of magnitude. Despite these differences with respect to S_1 and S_2, in all cases the largest attainable values of the fixed Δt correspond to methods with order higher than two, obtaining therefore more accurate solutions in less time. Again, this behavior can be related with that observed in [2] for the one dimensional linear advection-diffusion problem. In the regime where the explicit term starts to dominate (and this occurs in the *Q*-explicit and *Q*-splitting methods for the cases S_1,

S_2 and in the Q-implicit method for the case S_3), larger Δt were obtained for the IMEX-BDF schemes of orders 3 and 4 rather than for order 2.

5 Conclusions

In the time integration study [6] of the thermal convection in fast rotating fluid spherical shells, the possibility of handling implicitly the Coriolis term, and even the nonlinear term, thanks to the low memory requirements of the iterative Krylov methods used to solve the linear systems, was shown. That study focused on the influence of the Ekman number on the efficiency of the methods proposed. The present study extends the previous one by analyzing the influence of the Prandtl and the Rayleigh numbers.

The results presented here, computed at low $E = 10^{-4}$, show that the behavior of the methods for integrating a weakly supercritical oscillatory type of solution (periodic S_1 or quasiperiodic S_2) is very similar, despite their Prandtl number differ in one order of magnitude. At this regime, the Ekman number plays a major role, and a more implicit treatment of the Coriolis term becomes appropriate. In contrast, at strongly supercritical regime (S_3), an implicit treatment of the Coriolis term does not improve the integration, reflecting that the Ekman number plays a minor role. The solutions are obtained with less accuracy, reflecting their spatio-temporal chaotic character.

In all cases (S_1, S_2, and S_3) shown here (and also in the cases of [6]), the implementation of high order methods does not reduce the efficiency of the time integrators, and allows to obtain more accurate solutions. In addition, for the Q-splitting or Q-explicit fixed-step methods the largest time-steps are obtained with order higher than two, as occurs with the IMEX-BDF schemes applied in [2] to the one dimensional linear advection-diffusion problem when the dominant term of the equation is handled explicitly.

In practice the most efficient method depends strongly on R (also on E), but more weakly on σ, at least in the oscillatory regime. It depends also on the errors accepted for a solution, and on the type of solution. For instance, if one is just interested in obtaining solutions by direct numerical simulations (DNS), the best choice is to implement a fourth order Q-splitting method, and performing some previous experiments to determine the optimal time step. However, if the time integration is part of a continuation process, and/or one is interested in calculating the stability of the solutions, low errors must be requested to the time integration. Then the Q-implicit VSVO method will probably be the most efficient option. Moreover, since the lower run times correspond to the Q-implicit VSVO method with high tolerances, it might also be useful to pass long uninteresting transients, where having a control of the time stepsize might be important.

The results presented in this paper suggest that IMEX methods could also be efficiently used in other type of nonlinear problems with other spatial discretizations if the stiff part can be included in the implicit term of the scheme, and the cost of solv-

ing the corresponding linear systems, whatever their structure, becomes comparable to the evaluation of the explicit part.

6 ACKNOWLEDGEMENTS

This research has been supported by Spain Ministerio de Ciencia e Innovación, and Generalitat de Catalunya under projects MTM2010-16930 and 2009-SGR-67, respectively.

References

1. Ascher, U.M., Ruuth, S.J., Spiteri, R.J.: Implicit-explicit Runge-Kutta methods for time-dependent partial differential equations. Applied Numerical Mathematics **25**, 151–167 (1997)
2. Ascher, U.M., Ruuth, S.J., Wetton, B.T.R.: Implicit-explicit methods for time-dependent partial differential equations. SIAM J. Numer. Anal. **32**(3), 797–823 (1995)
3. Canuto, C., Hussaini, M.Y., Quarteroni, A., Zang, T.A.: Spectral Methods in Fluid Dynamics. Springer (1988)
4. Christensen, U.: Zonal flow driven by strongly supercritical convection in rotating spherical shells. J. Fluid Mech. **470**, 115–133 (2002)
5. Curtiss, C.F., Hirschfelder, J.O.: Integration of stiff equations. PNASUSA **38**, 235–243 (1952)
6. Garcia, F., Net, M., García-Archilla, B., Sánchez, J.: A comparison of high-order time integrators for thermal convection in rotating spherical shells. J. Comput. Phys. **229**, 7997–8010 (2010)
7. Garcia, F., Sánchez, J., Net, M.: Antisymmetric polar modes of thermal convection in rotating spherical fluid shells at high Taylor numbers. Phys. Rev. Lett. **101**, 194,501–(1–4) (2008)
8. Glatzmaier, G.: Numerical simulations of stellar convective dynamos. I. The model and method. J. Comput. Phys. **55**, 461–484 (1984)
9. Hairer, E., Norsett, H.P., Wanner, G.: Solving Ordinary Differential Equations. I Nonstiff Problems (2nd. Revised Edition). Springer-Verlag (1993)
10. Hindmarsh, A.C.: ODEPACK, a systematized collection of ODE solvers. In: R.S.S. et al. (ed.) Scientific Computing, pp. 55–364. North-Holland, Amsterdam (1983)
11. Net, M., Garcia, F., Sánchez, J.: On the onset of low-Prandtl-number convection in rotating spherical shells: non-slip boundary conditions. J. Fluid Mech. **601**, 317–337 (2008)
12. Pino, D., Mercader, I., Net, M.: Thermal and inertial modes of convection in a rapidly rotating annulus. Phys. Rev. E **61**(2), 1507–1517 (2000)
13. Plaut, E., Busse, F.H.: Multicellular convection in rotating annuli. J. Fluid Mech. **528**, 119–133 (2005)
14. Saad, Y., Schultz, M.H.: GMRES: a generalized minimal residual algorithm for solving non-symmetric linear systems. SIAM J. Sci. Stat. Comput. **7**, 865–869 (1986)
15. Sánchez, J., Net, M., García-Archilla, B., Simó, C.: Newton-Krylov continuation of periodic orbits for Navier-Stokes flows. J. Comput. Phys. **201**(1), 13–33 (2004)
16. Sánchez, J., Net, M., Simó, C.: Computation of invariant tori by Newton-Krylov methods in large-scale dissipative systems. Physica D **239**, 123–133 (2010)
17. Simitev, R., Busse, F.H.: Patterns of convection in rotating spherical shells. New Journal of Physics **5**, 97.1–97.20 (2003). DOI 10.1088/1367-2630/5/1/397
18. Tilgner, A.: Spectral methods for the simulation of incompressible flow in spherical shells. Int. J. Num. Meth. Fluids **30**, 713–724 (1999)